Magnetic Resonance and Microfluidics
Marcel Utz, *et al.*
Science **330**, 1056 (2010);
DOI: 10.1126/science.1198402

in *PSEN1* produce different clinical phenotypes, hinting at different disease mechanisms. Although Notch1 appears to be the relevant substrate for γ-secretase in acne inversa, it is unclear whether Notch1 is involved in presenilin-dependent neuronal survival in the aging brain. The absence of dementia in the families with acne inversa also indicates that *PSEN1* haploinsufficiency is unlikely to cause familial Alzheimer's disease, although the acne inversa–affected family transmitting the *PSEN1* mutation includes just four affected individuals, and delayed onset and/or subtle signs of dementia cannot be excluded.

Conversely, Wang *et al*. note that acne inversa has not been reported in association with Alzheimer's disease, which is surprising given the 1 to 4% prevalence of acne inversa in the general population (*9*). Moreover, some *PSEN1* mutations in familial Alzheimer's disease cause a complete loss of Notch1 processing in cultured cells (*10*), which would be expected to mimic the phenotypic effects of the *PSEN1* mutation in familial acne inversa. In addition, loss of a single *Psen1* allele in mice does not produce skin disorders, which occur only with more severe reductions of presenilin expression. These inconsistencies raise the possibility that loss-of-function mutations in *PSEN1* may not always produce acne inversa with full penetrance, and that genetic modifiers may contribute to the development of acne inversa in the reported families.

Although *PSEN* mutations in familial Alzheimer's disease impair protein function, the missense nature of these mutations suggests that expression of the mutant protein is necessary to produce the disease. *PSEN* mutations could enhance production of longer Aβ by decreasing the proteolytic efficiency of the mutant protein (*11*). This model, however, is not compatible with the inability of presenilins bearing some pathogenic mutations to generate Aβ (*12*). Alternatively, mutant presenilin could influence the activity of wild-type presenilin in a dominant-negative manner (*2*). Such a "gain of negative function" model would reconcile the dominant inheritance of *PSEN* mutations with their deleterious effects on protein function. That presenilin is the only γ-secretase subunit targeted by mutations in familial Alzheimer's disease further suggests that γ-secretase–independent functions of presenilins may be important in disease pathogenesis. Presenilins are required for synaptic function and neuronal survival in the adult brain (*4*, *13*), establishing important links to neural processes perturbed in Alzheimer's disease, but the effector mechanisms mediating these essential activities are presently unclear.

A large-scale phase III clinical trial of a γ-secretase inhibitor (semagacestat) in Alzheimer's disease was halted because the drug worsened cognition and increased the risk of skin cancer (*14*). Mouse studies suggest that these adverse effects may be attributed to specific inhibition of γ-secretase rather than to nonspecific effects. The dementia and neurodegeneration caused by presenilin inactivation in the mouse brain predicted that γ-secretase inhibition might exacerbate the clinical features of Alzheimer's disease (*4*). In addition, reduced γ-secretase and Notch1 activity in mice causes a high frequency of skin cancer, demonstrating that γ-secretase is a tumor suppressor in skin (*6*–*8*). It remains to be seen whether the adverse effects of γ-secretase inhibitors include acne inversa.

The findings by Wang *et al*. should spur efforts to dissect the role of γ-secretase in acne inversa, and to examine patients with acne inversa and familial Alzheimer's disease more closely for evidence of subtle overlap in the clinical features. Better understanding of the molecular mechanisms by which presenilin and γ-secretase dysfunction leads to these disparate conditions will also bolster efforts to devise safe and effective disease-modifying therapies.

References

1. B. Wang *et al*., *Science* **330**, 1065 (2010).
2. J. Shen, R. J. Kelleher III, *Proc. Natl. Acad. Sci. U.S.A.* **104**, 403 (2007).
3. J. Hardy, D. J. Selkoe, *Science* **297**, 353 (2002).
4. C. A. Saura *et al*., *Neuron* **42**, 23 (2004).
5. M. C. Irizarry *et al*., *J. Neurosci.* **17**, 7053 (1997).
6. X. Xia *et al*., *Proc. Natl. Acad. Sci. U.S.A.* **98**, 10863 (2001).
7. T. Li *et al*., *J. Biol. Chem.* **282**, 32264 (2007).
8. M. Nicolas *et al*., *Nat. Genet.* **33**, 416 (2003).
9. F. W. Danby, L. J. Margesson, *Dermatol. Clin.* **28**, 779 (2010).
10. W. Song *et al*., *Proc. Natl. Acad. Sci. U.S.A.* **96**, 6959 (1999).
11. M. S. Wolfe, *EMBO Rep.* **8**, 136 (2007).
12. E. A. Heilig, W. Xia, J. Shen, R. J. Kelleher III, *J. Biol. Chem.* **285**, 22350 (2010).
13. C. Zhang *et al*., *Nature* **460**, 632 (2009).
14. http://newsroom.lilly.com/releasedetail.cfm?releaseID=499794, accessed on 10 October 2010.

10.1126/science.1198668

CHEMISTRY

Magnetic Resonance and Microfluidics

Marcel Utz[1,2] and James Landers[2,1]

The inner workings of microscale "lab-on-a-chip" devices can be revealed by nuclear magnetic resonance measurements on their exiting fluid flows.

Magnetic resonance imaging (MRI) is a well-established clinical tool that is routinely used to locate cartilage or ligament damage, cancerous lesions, and blood vessel occlusions; when combined with magnetic resonance spectroscopy (MRS), it can even map brain function. The image contrast in MRI instruments comes from the change in orientation of the rotational axis (precession) of atomic nuclei in a magnetic field, and can be adjusted to selectively image tissues on the basis of oxygen content, diffusivity, flow velocity, and other properties. Microfluidic "lab-on-a-chip" (LOC) devices represent an emerging technology with potential applications in medical diagnostics. These devices flow samples (which often consist of suspensions of cells) and reagents through miniaturized chemical reactors, and are typically fabricated via lithographic methods similar to those used in microelectronics. Although in principle, MRI should be the ideal tool for monitoring reactions on LOC devices, in practice this turns out to be notoriously difficult because of limitations in sensitivity and resolution. On page 1078 of this issue, Bajaj *et al*. (*1*) present an ingenious method that allows sensitive MRI measurements on an LOC device by recording magnetic resonance signals from the spent fluid that exits the device.

In MRI, the spatial position of a spin can be inferred from changes in its precession frequency. The sample is placed in a magnetic field that has a gradient in one direction. The nuclear spins are excited by radio-frequency pulses, and the resulting Larmor precession induces a signal in a receiver coil surrounding the sample. The field gradient causes the precession frequency of each spin to depend on its location. The experiment is repeated

[1]Department of Chemistry, University of Virginia, Charlottesville, VA 22904, USA. [2]Department of Mechanical and Aerospace Engineering, University of Virginia, Charlottesville, VA 22904, USA. E-mail: mu3q@virginia.edu; jpl5e@virginia.edu

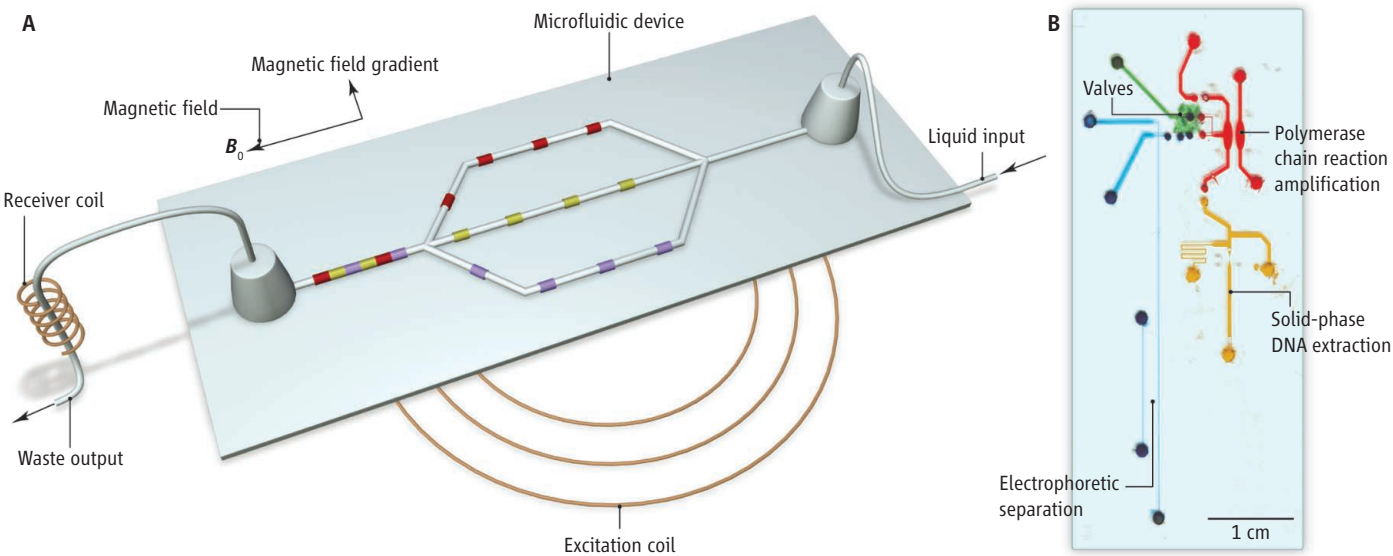

The answers flow out in the end. (**A**) Principles of remote detection of processes inside microfluidic devices with MRI are illustrated. Spin precession is induced in the entire chip by means of the excitation coil. Liquid is pumped through the microfluidic chip. Volume packets flowing through different channels in the network precess at different frequencies because of a gradient in the magnetic field (represented by red, green, and violet colors in the channels). The phase angle acquired in this precession is converted into a modulation of the spin polarization, which is long-lived. The labeled volume packets are then transported to the receiver coil, where the information is read out. (**B**) The photo shows an integrated microfluidic chip for genomics that analyzes short tandem repeats.

with a field gradient of different magnitude and direction, and an image is obtained by Fourier transformation of the resulting data set. Special pulse-excitation protocols can encode additional parameters, such as velocity and diffusivity.

Microfluidic LOC devices consist of networks of channels, chambers, and valves with features that range in size from hundreds of nanometers to a few millimeters (*2*–*4*). Compared with benchtop methods, LOCs require very small volumes of samples and reagents, and create a closed system that minimizes the risk of contamination. Complex analytical methods can be brought directly into the hands of forensic, environmental, and other scientists, as well as primary medical care providers, even in remote locations far from sophisticated laboratory facilities.

The key processes that occur within an LOC—fluid convection (flow), diffusion, separation, and chemical reactions—can all be monitored with MRI and MRS, even simultaneously. Other flow quantification methods, such as optical particle tracking, perturb the system and provide no chemical information. Because MRI uses the atomic nuclei as "spies" to convey information about the chemical and transport processes, it causes no such perturbation. Unfortunately, MRS and MRI both suffer from low sensitivity. A sample contained within the small internal structures of an LOC device poses a challenge because the strength of the induced signal per spin decreases as the coil size is increased to accommodate the device.

Past endeavors to combine magnetic resonance with microfluidic systems have resorted to miniaturized receiver coils (*5*–*8*) or microstrip lines (*9*, *10*) that focus the sensitivity on the available sample volume. This approach has led to "hyphenated" techniques, such as liquid chromatography–magnetic resonance (*11*). By integrating planar microcoils onto the chip (*6*–*8*), the products of on-chip reactions and separations can be quantified by MRS. The coils can be coupled wirelessly to the MRS receiver so that data can be collected without needing physical connections, by simply inserting the chip into the MRI scanner (*7*, *8*). However, the operation of the microfluidic system as a whole cannot be observed through such focused receivers, because it is impractical to envelop each pertinent feature with a separate microcoil.

Bajaj *et al*. have circumvented the dilemma between receiver sensitivity and size. As in conventional MRI, they used magnetic-field gradients to encode position and velocity, exciting nuclear precession with a large radio-frequency coil that surrounds the entire LOC. However, leveraging a development by the Pines group several years ago (*12*) to study the flow of gases in porous media (*13*), the frequency is measured only after the polarized nuclei have been washed out of the LOC along with the surrounding fluid, into an exit microcapillary wound with a small receiver coil (see the figure, panel A). With the resulting optimum sensitivity, transport processes in microfluidic systems can be observed directly that would otherwise have been inaccessible.

In a sense, this approach is similar to a recently proposed method (*14*) that injects dyes into different parts of the chip, which are then detected by absorbance spectroscopy from a common exit port; instead of dyes, the more elegant MRI approach by Bajaj *et al*. uses nuclear spin states as tracers. The only requirement for investigating an LOC in this way is that the spins are transported to the observation coil within the spin-lattice relaxation time, usually several seconds. It should be possible to study most LOCs, given typical pumping speeds and small device length scales. Obviously, such measurements require fluidic connections to the chip while it is in the MRI scanner to ensure continued flow. This restriction notwithstanding, it is exciting that the broad arsenal of MRI techniques is now available to study chemical reactions, separation, convection, and diffusion processes in LOC devices.

An example of an LOC that could be examined—a genomic analysis chip that integrates cell lysis, DNA purification, polymerase chain reaction amplification, and electrophoretic separation (*3*)—is shown in panel B of the figure. It contains a host of elements that rely on complex transport and separation processes (indicated by the arrows), which could, in principle, be studied by MRI.

With the work of Bajaj *et al*., it now seems justified to hope that MRI will be able to do

CREDIT (PANEL A): P. HUEY/*SCIENCE*

Published by AAAS

for the development of microfluidic LOCs what it has done for medical diagnostics, by providing a generally applicable, powerful, and flexible tool to study a complex chemical and biological system without perturbing its operation.

References

1. V. S. Bajaj, J. Paulsen, E. Harel, A. Pines, *Science* **330**, 1078 (2010).
2. T. Thorsen *et al.*, *Science* **298**, 580 (2002).
3. C. J. Easley *et al.*, *Proc. Natl. Acad. Sci. U.S.A.* **103**, 19272 (2006).
4. R. G. Blazej, P. Kumaresan, R. A. Mathies, *Proc. Natl. Acad. Sci. U.S.A.* **103**, 7240 (2006).
5. D. L. Olson, T. L. Peck, A. G. Webb, R. L. Magin, J. V. Sweedler, *Science* **270**, 1967 (1995).
6. C. Massin *et al.*, *J. Magn. Reson.* **164**, 242 (2003).
7. M. Utz, R. Monazami, *J. Magn. Reson.* **198**, 132 (2009).
8. M. Utz, K. Wang, in *Proceedings of the 13th International Conference on Miniaturized Systems for Chemistry and Life Sciences (μTAS 2009)*, Jeju, Korea, 1 to 5 November, 2009, T. S. Kim *et al.*, Eds. (Chemical and Biological Microsystems Society, San Diego, 2009), p. 1656.
9. H. G. Krojanski, J. Lambert, Y. Gerikalan, D. Suter, R. Hergenröder, *Anal. Chem.* **80**, 8668 (2008).
10. J. Bart, J. W. Janssen, P. J. van Bentum, A. P. Kentgens, J. G. Gardeniers, *J. Magn. Reson.* **201**, 175 (2009).
11. K. Albert, Ed., *On-line LC-NMR and Related Techniques* (Wiley, Chichester, UK, 2002).
12. J. Granwehr, E. Harel, S. Han, S. Garcia, A. Pines, *Phys. Rev. Lett.* **95**, 07553 (2004).
13. C. Hilty *et al.*, *Proc. Natl. Acad. Sci. U.S.A.* **102**, 14960 (2005).
14. D. C. Leslie *et al.*, *Lab Chip* **10**, 1960 (2010).

10.1126/science.1198402

MICROBIOLOGY

Topping Off a Multiscale Balancing Act

Quantitative predictions of the relationship between cell growth and gene expression have been made and validated in *Escherichia coli*.

Joshua Lerman and Bernhard O. Palsson

The genotype-phenotype relationship is fundamental to biology. Finding general, underlying rules that govern the complex relationship between gene expression and cell growth, however, has proven a challenge. On page 1099 of this issue, Scott *et al*. (*1*) offer empirical "growth laws" that correlate the growth rates of bacteria with how they allocate resources to protein synthesis and metabolic functions.

The genotype-phenotype relationship in microbes can be conceptualized as a five-layer hierarchical model (see the figure). A cell faces myriad constraints on its function at all layers (*2*, *3*). At the whole-cell level, it may be difficult to determine the constraints that govern cellular functions on a mechanistic basis, but they can be identified from empirical observation. Microbiologists pursued this approach in the 1950s and 1960s, resulting in empirical parameters such as the growth and nongrowth maintenance coefficients (*4*) and yield coefficients that are widely used in the bioprocessing literature (*5*).

Scott *et al*. expand on the whole-cell empirical approach by means of an insightful combination of targeted experimentation and mathematical analysis. Using *Escherichia coli* cells grown under a variety of conditions, they first confirmed a previously established correlation between growth rate and the ribosomal content of the cell (ribosomes assemble proteins from amino acids). Next, they used mutant strains to show that the proportionality constant between ribosomal content and growth rate depends on the overall rate at which the cell incorporates amino acids into protein. To achieve a small increase in growth rate, mutant strains that incorporate amino acids slowly must dedicate more resources to ribosome production than their more rapidly synthesizing counterparts.

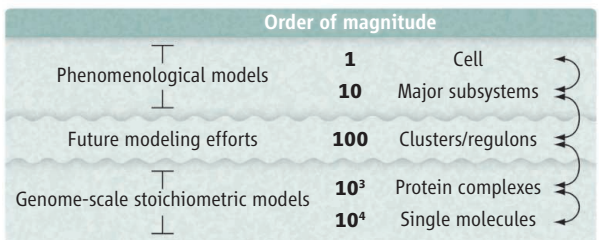

The microbial genotype-phenotype relationship. Bacterial cell growth and gene expression are linked through a hierarchy that extends from tens of thousands of molecules to a single cell. Each layer in the hierarchy imposes constraints on adjacent layers (arrows, right). At the top, empirical models can predict the relative levels of proteins belonging to major subsystems within a cell (e.g., metabolism, macromolecular synthesis). At the bottom, genome-scale models can make predictions by accounting for all single molecules and protein complexes. A future modeling challenge is to characterize the functionality of the ~100 coordinately expressed clusters of protein complexes and to determine the evolutionary pressures leading to regulon formation (middle layer).

The authors then subjected cells growing in different nutritional environments to increasing concentrations of an antibiotic that disables ribosomal function. Another striking correlation emerged: As the concentration of the antibiotic increased, translation capacity and growth dropped linearly toward zero, and there was a corresponding linear increase in the fraction of the proteome dedicated to ribosomes. Finally, chemical composition data taken from cells close to the no-growth point suggested that there is a hard upper bound on the fraction of the proteome that can be dedicated to ribosomes and related proteins; it is capped at around 0.55, independent of growth conditions.

Given these findings, and given that the cell's regulatory efforts enforce a balance between metabolism and macromolecular synthesis, the authors reasoned that they could mathematically describe proteome resource allocation using only three variables: R, P, and Q, where R represents the growth rate–dependent fraction of the proteome that is dedicated to macromolecular synthesis, P represents the growth rate–dependent fraction of the proteome dedicated to everything else, and Q represents the growth rate–independent (or housekeeping) fraction. This grouping of proteins into three categories is able to relate R, P, and Q in quantitative terms without any adjustable parameters, and without requiring detailed knowledge of the underlying regulatory circuits. Surprisingly, Q-class proteins occupy a substantial fraction of the proteome (50%).

The authors evaluated the predictive potential of these empirical equations through a series of experiments. They exploited the empirical relationships between proteome fractions to (i) validate the predicted constrained positive linear relationship between the abundance of P-class proteins and growth rate in a fixed nutritional environment, and (ii) mathematically characterize cells forced to express unnecessary (or useless) protein.

This work comes on the heels of parallel developments at lower levels of the hierarchy shown in the figure. The availability of

Department of Bioengineering, University of California, San Diego, La Jolla, CA 92093, USA. E-mail: palsson@ucsd.edu